

# Oxidation Behavior of Nanostructure CrAlN Thin Films

Adisorn Buranawong, Nirun Witit-anun\*

Material Innovation Research Laboratory, Department of Physics, Faculty of Science, Burapha University, Chonburi 20131

\*Corresponding author e-mail: nirun@buu.ac.th

Received: 18 May 2024 / Revised: 1 August 2024 / Accepted: 12 February 2025

## Abstract

In this research, the nanostructure chromium aluminium nitride (CrAlN) thin films were prepared on silicon (100) substrate by reactive DC magnetron sputtering technique with Cr-Al alloy target and then annealing in air at different temperatures (500-900°C) to investigate the oxidation behavior. The films' oxidation rate and oxidation activation energy were also calculated using parabolic relations and the Arrhenius equation. The X-ray diffraction (XRD) indicated that a solid solution CrAlN structure was found for the as-deposited thin film whereas the mixed oxide phase of Cr<sub>2</sub>O<sub>3</sub> and Cr<sub>5</sub>O<sub>12</sub> structures were discovered in the XRD spectra upon oxidation temperature at 800°C. The Energy dispersive X-ray spectroscopy (EDS) examination demonstrated the obvious increase of oxygen concentration at oxidation temperature from 800°C due to the oxidation mechanism. The oxidation behavior was also confirmed by field-emission scanning electron microscopy (FE-SEM) analysis which the grain aggregation was observed while the cross-sectional microstructure of the thin films revealed that a very thin dense oxide layer was formed on the CrAlN layer. The oxide thickness increased from 648 nm to 1044 nm with increasing annealing temperature. The thin films began oxidizing above 800°C, resulting in a porous structure. It was discovered that the as-deposited thin film exhibited a high-temperature oxidation resistance at 800°C. The oxidation rate increased from  $1.43 \times 10^{-13}$  to  $3.78 \times 10^{-13}$  cm/s<sup>2</sup> and was obtained from an annealing temperature of 800°C. The oxidation activation energy calculated from the Arrhenius plot was 99.85 kJ/mol. The nanoindentation technique also reported that the hardness of the films decreased from 15.92 to 0.03 GPa through the annealing temperature.

**Keywords:** Oxidation behavior, CrAlN, Thin film, Sputtering, Alloy target

## 1. Introduction

Hard coatings and wear-resistant coatings using transition metal nitride of CrN have always attracted much attention for many decades (Alaksanasuwan et al., 2022; He et al., 2000; Qu et al., 2023; Xingrun, Qinying, et al., 2018). However, during use, oxidation at high temperatures unavoidably causes the coatings to deteriorate. The ability of coatings to oxidize is one of the crucial elements for effective application. There have been numerous oxidation investigations on CrN coatings conducted in the past (Kang et al., 2021; Liu et al., 2021; Qi et al., 2013) but the oxidation limit of CrN coating is typically thought to be after 600°C (He et al., 2021; Khamseh & Araghi, 2016).

CrAlN thin films are well-known used for replaced CrN thin films due to their high toughness, high compressive residual stress, excellent film adhesion, high anti-oxidation temperature high mechanical properties, and wear resistance (Khamseh et al., 2010; Tillmann et al., 2018; Xingrun, Zhu, et al., 2018). In the case of cutting and machining tools, they must not only have extreme mechanical properties, but they must also be resistant to potentially hostile operating environments such as lubricant, cooling solutions, and high temperatures (Khamseh, Nose, Kawabata, Matsuda, & Ikeno, 2010; Mayrhofer et al., 2008). As a result, the protective coating used must be able to endure such harsh conditions. CrAlN film is the most promising nitride for use as a protective film compared to the CrN film because of its great oxidation resistance due to the production of complex aluminum and chromium oxides contributes to the formation of a dense mixed oxide layer of Cr<sub>2</sub>O<sub>3</sub> and Al<sub>2</sub>O<sub>3</sub> on the film's surface (Zhang et al., 2008) which prevents further diffusion of oxygen into the film bulk (Banakh et al., 2003).

Reactive Magnetron Sputtering is a Physical Vapor Deposition (PVD) technique which most favorable used for depositing both of binary (TiN, CrN, ZrN) or ternary (TiCrN, CrAlN, CrZrN) hard coatings (Alaksanasuwan et al., 2022; Alaksanasuwan, & Witit-anun, 2023). The CrAlN is one of the most interesting ternary hard coatings due to the high uniformity, high hardness, and show better adherence to the substrate (Anwar et al., 2022; Priyadarshini et al., 2023). The majority of CrAlN film has so far been deposited using a co-sputtering target. This

approach has the drawback of requiring simultaneous control of many targets (Kim et al., 2021), which eventually have many power supplies in the deposition system whereas a single alloy target can overcome this problem because simplify the sputtering process by using only one power supply for the sputtering process.

The oxidation behavior of CrAlN thin films prepared using co-target, whose oxidation limit was determined to be in the range of 800°C to 1000°C was also thoroughly investigated from previous literature (Kayani et al., 2006; Khamseh, Nose, Kawabata, Matsuda, & Ikeno, 2010; Lin et al., 2008; Zhu et al., 2006) for example, Lin et al. (2008) were found that CrAlN coatings which deposited by magnetron sputtering technique, the corresponding oxidation reactions and structural changes during the thermal oxidation process, exhibit good thermal stability up to 900°C in air and forming dense (Cr,Al)<sub>2</sub>O<sub>3</sub> oxide layer on the film surface. However, relatively few oxidation investigations on CrAlN thin films produced by magnetron sputtering with a Cr-Al Alloy target have been conducted. Therefore, more detailed studies including the oxidation behavior and the oxidation mechanism under various oxidizing temperatures are still needed to fulfill. The purpose of this research was to investigate the oxidation behavior of CrAlN thin films sputtered from the Cr-Al alloy target.

## 2. Materials and Methods

### 2.1 Preparation of thin film

A thin film of CrAlN was deposited on a silicon (100) plane substrate. A homemade DC magnetron sputtering system was used to deposit the film using a single high-purity of CrAl alloy target. Before loading the silicon substrates into the deposition chamber, they were ultrasonically cleaned in acetone and ethyl alcohol, sequentially for 10 min. The chamber was equipped with a diffusion pump and a rotary pump. The chamber was pumped down to  $5 \times 10^{-5}$  mbar before began deposition process. The deposition parameters of the CrAlN thin films were listed in Table 1, after that, the films were annealed at various temperatures to investigate the oxidation behavior.

**Table 1.** Thin films deposition conditions.

Parameters	Details
Sputtering target	Cr-Al alloy
Substrate temperature	room temperature
Target to substrate distance	100 mm
Base pressure	$3.0 \times 10^{-5}$ mbar
Working pressure	$5.0 \times 10^{-3}$ mbar
Sputtering power	230 W
Ar flow rate	2 sccm
N <sub>2</sub> flow rates	6 sccm
Deposition time	30 min

### 2.2 Oxidation behavior investigation

The as-deposited CrAlN film was thermally oxidized in a temperature-controlled standard furnace (CARBOLITE, CWF1300) with no additional features to control humidity or air flow rate. At the center of the furnace, samples were placed horizontally on a ceramic holder with the coated face up. The furnace temperature was electronically controlled and raised to the desired annealing temperature varied from 500-900°C. The annealing time was set to yield a total oxidation period of one hour. The furnace was gradually cooled to ambient temperature after each interval of annealing temperature.

After the annealing process, the film's oxidation behavior was detected by the following techniques as follows, an X-ray diffractometer (XRD) (Bruker, D8 Advance) was used to determine the crystal structure of the films before and after annealing. Scans were performed with the thin film goniometer in the grazing angle mode with an incident beam angle of 3° from 20° to 80° of a 2θ range with a scanning speed of 2° min<sup>-1</sup>.

Energy dispersive X-ray spectroscopy (EDS) (EDAX) which is equipped in a Scanning Electron Microscope (LEO, 1450VP) was used to measure the chemical compositions of the films. A high-resolution scan of the plane view and cross-sectional analysis of morphology and oxide layer on the film's surface was provided using field-emission scanning electron microscopy (FE-SEM) (Hitachi, S-4700).

A nanoindentation instrument (Bruker, Hysitron TI Premier) was used to measure the hardness at various annealing temperatures. The load was chosen to maintain an imprint depth of no more than 10% of film thickness, allowing the influence of the substrate to be ignored.

The oxidation rate constant ( $k_p(T)$ ) and oxidation activation energy ( $E_a$ ) of the as-deposited films at a specific temperature has been used to describe oxidation behavior following a parabolic relation (Buranawong & Witit-anun, 2022). The Wagner's parabolic oxidation relation, which is typically used to describe the oxidation rate, which is defined as the growth of an oxide film by thermal oxidation. The Arrhenius plot was used to calculate the oxidation activation energy.

### 3. Results and Discussion

#### 3.1 Crystal structure of oxide phase

Figure 1 depicts the X-ray diffraction-identified crystal structure and phase of the film both as-deposited and after 1 hour of oxidation at various temperatures in the air. It exhibited no XRD pattern with a wide dome found between diffraction angles from  $35.00^\circ$  to  $50.00^\circ$  for the as-deposited films.

The diffraction angle was from  $35.00^\circ$  to  $50.00^\circ$  which varied between standard CrN (JCPDS No.65-2899) and AlN (JCPDS No.88-2250) the film's crystal structures were identified when annealed the films between  $500-700^\circ\text{C}$ . This result can conclude that the film was the solid solution of CrAlN crystal structure with (200) plane. The x-ray diffraction pattern was also did not found any of the oxide compounds that occurred from the oxidation mechanism.

As  $800^\circ\text{C}$ , various of crystal structures were exhibited. The CrAlN structure (200) plane was also found whereas the x-ray intensity was significantly increased. The additional of the  $2\theta$  peak at  $26.90^\circ$ ,  $40.90^\circ$ , and  $49.75^\circ$  were exhibited. This result was in good agreement with the JCPDS standard (No.73-1787) for the orthorhombic  $\text{Cr}_5\text{O}_{12}$  structure as (311), (123) and (024) planes. The  $2\theta$  at  $36.20^\circ$ ,  $72.83^\circ$ , and  $74.82^\circ$  which correspond to the JCPDS standard of  $\text{Cr}_2\text{O}_3$  rhombohedral structure (No.82-1484) as (110), (1010) and (119) planes were identified. However, a strong preferred orientation was exhibited for the CrAlN (200) plane.

At an oxidation temperature of  $900^\circ\text{C}$ , resulted is no change for all peaks of each crystal structure. The polycrystalline  $\text{Cr}_5\text{O}_{12}$  and  $\text{Cr}_2\text{O}_3$  structures mixed with CrAlN structures have remained. Additionally, the XRD pattern was used to determine the crystallite size of the CrAlN peak, which was calculated using Scherrer's equation. As the oxidation temperature rose from  $500$  to  $900^\circ\text{C}$ , the crystal size increased from  $8.4$  to  $23.7$  nm.

It can be concluded that the crystal structure revolution from the oxidation mechanism was investigated before and after annealing the as-deposited thin films. The as-deposited thin film was performed an amorphous structure and at an oxidation temperature from  $500$  to  $700^\circ\text{C}$ , the crystal structure of the films was changed to CrAlN (200) plane crystal structure. In this study, a transition region of crystal structural transformations was identified. When further increased annealing temperature, the CrAlN thin films started to transform into a mixed oxide compound of  $\text{Cr}_5\text{O}_{12}$  and  $\text{Cr}_2\text{O}_3$  with orthorhombic and rhombohedral structures, respectively, at an oxidation temperature between  $800$  and  $900^\circ\text{C}$ . It was implied that a small fraction of the film starts oxidized at  $800^\circ\text{C}$  therefore, the films performed oxidation resistance at  $700^\circ\text{C}$ .

This result suggests that oxygen from the annealing atmosphere reacts with the Cr atom in the CrAlN thin films resulting in the formation of chromium oxide compounds with  $\text{Cr}_5\text{O}_{12}$  and  $\text{Cr}_2\text{O}_3$  crystal structures through oxidation mechanisms (Lin et al., 2008). The transformation of the solid solution into the  $\text{Cr}_5\text{O}_{12}$  and  $\text{Cr}_2\text{O}_3$  phases observed in this study were consistent with the results of the previous literature (Barshilia et al., 2006; Khamseh et al., 2010; Lin et al., 2008). The XRD investigation indicated that the oxidation resistance temperature of the CrAlN thin films was  $700^\circ\text{C}$ . This result was consistent with the other researchers who found that the CrAlN thin films started to oxidize at an annealing temperature of over  $700^\circ\text{C}$  (Chim et al., 2009).

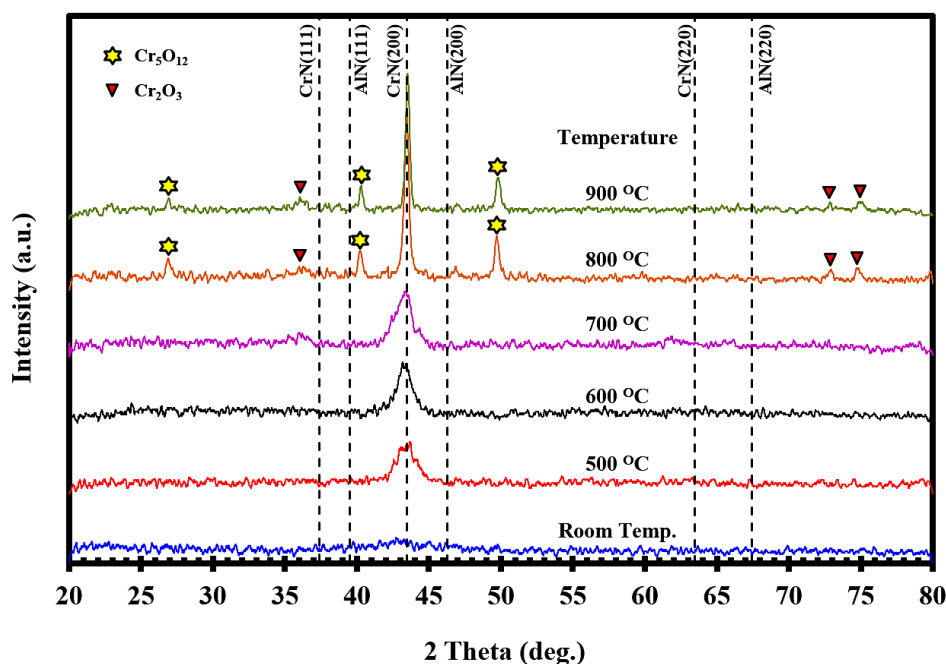


Figure 1. XRD pattern of CrAlN thin films at different annealing temperature.

### 3.2 Element compositions of oxide scale

For the element composition analysis by EDS technique was used to investigate the Cr, Al, N content, especially to detect the composition of the O which indicated oxidation behavior listed in Table 2. The result shows the Cr, Al, N, and O contents were changed as a function of the annealing temperature from 500 to 900°C.

The Cr, Al, N, and O content were 28.46, 30.93, 29.17, and 11.43 at%, respectively, at the as-deposited thin films. A gradual increase of O content from 13.80 to 20.06 at% but a slightly decrease of Cr, Al, and N contents from 29.22 to 25.00 at%, 31.29 to 29.48 at%, and 25.69 to 25.47 at%, respectively, were found after annealed from 500 to 700°C. With further increases in annealing temperature to 800 and 900°C, the O content was significantly increased to 42.88 at% whereas the rapid decrease of Cr and N contents to 11.52 at% and 17.73 at% were observed. In addition, there is not much decrease of Al content.

The results indicated that the O contents were governed by annealing temperature which can investigate the oxidation behavior. There is experimental evidence of the presence of O content before and after annealing the film from 500 to 900°C. In the case of as-deposited thin films, a small O content was observed due to oxygen from residual gas in the vacuum chamber. The O content also starts enhanced when increase annealing to 700°C. However, the oxidation of the film did not occur because no oxide compound was detected from the diffraction peak by using XRD.

It is clearly seen that with the extension of the annealing temperature from 800 to 900°C, the O content greatly increased compared to the lower annealing temperature (500-700°C). This evidence was in good agreement with the XRD analysis because a mixed structure of Cr<sub>5</sub>O<sub>12</sub> and Cr<sub>2</sub>O<sub>3</sub> phases was found. On the other hand, Cr, Al, and N contents were decreased as annealed the films. At 800-900°C, the films were oxidized by high thermal energy that induced the formation of an oxide compound. It has proven that the film performed oxidation resistance at 700°C which was confirmed by XRD and EDS.

### 3.3 Morphologies and cross-section of oxide scale

Figure 2 shows the FE-SEM micrographs of the surface morphology of the film through annealing temperature. The FE-SEM micrographs prove that the surface of the films composed of a small fine grain with a dense pattern spread across the surface was observed for the as-deposited film. The surface morphologies remained the same pattern until 700°C. Grains were found to coarsen with a rounded appearance shape on some areas of the film at 800°C. At 900°C, the formation of a needle-like structure with different sizes was observed.

The evolution of surface morphologies including can be clearly identified when the increased annealing temperature is over 700°C. Some area of the film surface was covered by an oxide layer due to a grain accommodation which was obtained at 800°C. The film surface is uniformly oxidized and covered by a needle-

like oxide layer, as can be seen in FE-SEM pictures of the surface after it has been annealed at 900°C. It can be concluded that grain characteristic that differs from the original appearance can be recognized as oxide compound grains (Khamseh et al., 2010; Zhang et al., 2008).

Moreover, the coarse grains (at 800°C) and needle-like shapes (at 900°C) are confirmed to be oxide compounds by the EDS analysis. It can prove that the CrAlN thin film, in this work, began oxidized at 800°C and still occurred at 900°C which also supports the oxidation behavior of the films that exhibited oxidation resistance at 700°C from XRD and EDS investigations. The increased O content with the oxidation mechanism of the films at elevated temperatures from this research was also in good agreement with other researchers (Chim et al., 2009).

Figure 3 shows the cross-sectional morphology and oxide layer of the film from the annealing process were evaluated to study the oxidation behavior. A very dense cross-sectional morphology can be observed for the as-deposited thin films (Figure 3). The grain aggregation with no void without the formation of an oxide layer was obtained as increased annealing temperature from 500 to 700°C. A cross-sectional structure was aligned with Zone T of the Thornton structure zone model (Anders, 2010).

The films exhibited a multilayer, 648 nm of oxide scale surface-layer, columnar with porous between grain boundary sub-layer, which can be seen at 800°C (Figure 3). The increase of oxide scale to 1044 nm, agglomeration of grain, and more void has occurred at 900°C whereas the decrease of CrAlN thickness. The appearance of the oxide layer and increased thickness which identified with the assistance of EDS due to the high O content. This result is also in agreement with the XRD results presented in Figure 1 as a result of oxide compound formation. It was confirmed that the film showed oxidation resistance at 700°C. This result was good agreement to the previous literature that the CrAlN thin film started to oxidize at 700°C (Chim et al., 2009).

This oxidation behavior can explain that the oxide scale of CrAlN coatings grows by simultaneous outward diffusion of Cr towards the oxide/air interface and inward diffusion of O to the oxide/nitride interface then N is released to the environment through some short diffusion paths in the oxide scale where the film is oxidized (Banakh et al., 2003).

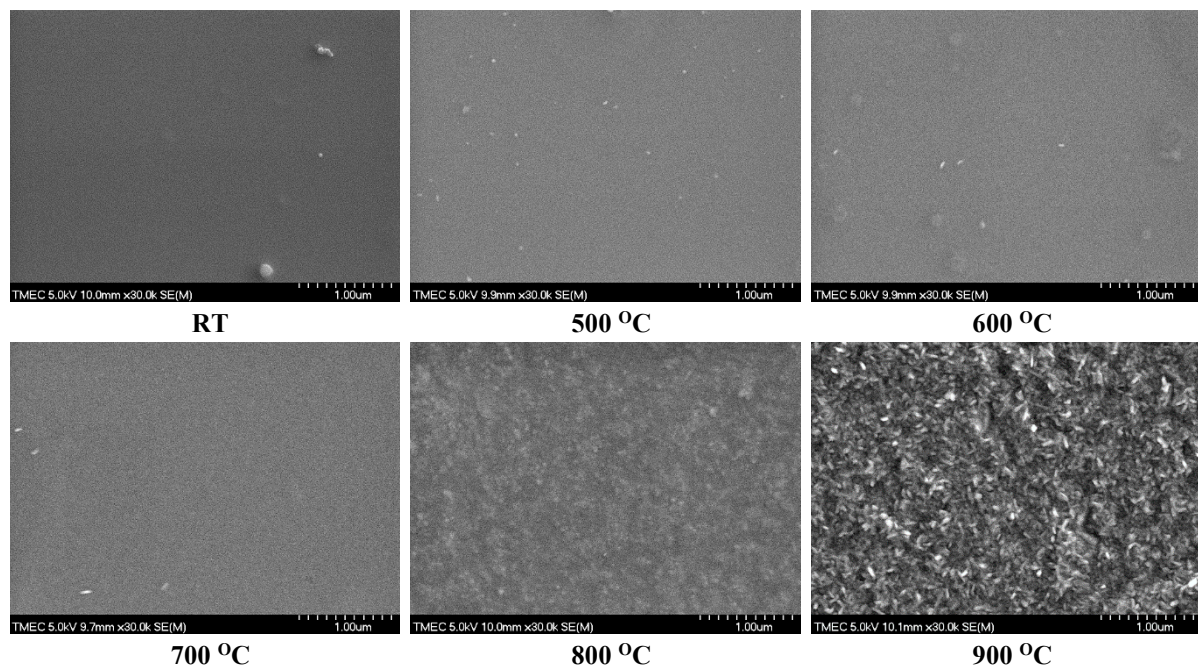


**Figure 2.** Surface morphology of CrAlN thin films at various annealing temperatures.

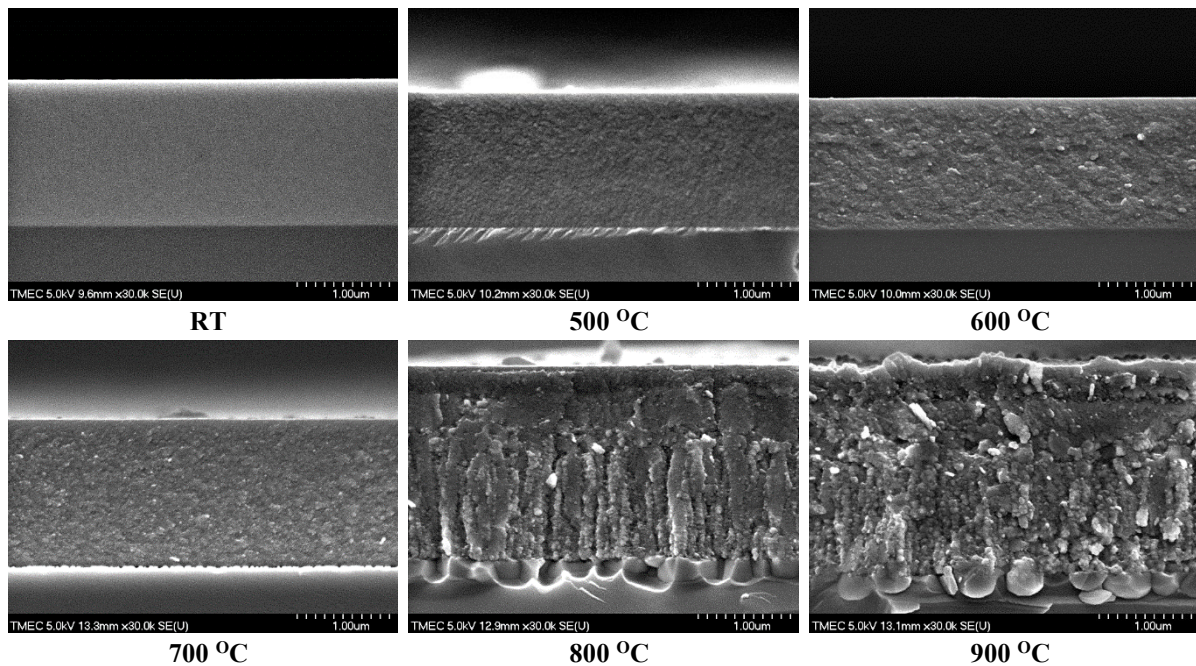


**Figure 3.** Cross-sectional of CrAlN thin films at various annealing temperatures.

### 3.4 Hardness of oxide scale

Test results are also summarized in Table 2. The hardness of films decreased with increasing temperature. The hardness of the as-deposited CrN coating is 12.47 GPa but recovery to 15.92 GPa at 500°C was measured. After annealing at 600 and 700°C the hardness was decreased to 11.16 and 7.23 GPa, respectively. The hardness of the annealed films above 700°C is still significantly drops to very low values, about 0.71 and 0.03 GPa at 800 and 900°C, respectively.

The recovery of the hardness of the film at 500°C may be due to the formation of Al<sub>2</sub>O<sub>3</sub> scale on the CrAlN surface, which could both retard the coating oxidation and contribute to the hardness recovery (Wang & Nie, 2014). However, the decrease of the hardness as further increased annealing temperature is attributed to the formation of thin and soft oxide layers on the surface of the coatings.

**Table 2.** Element compositions, film with oxide layer thicknesses, oxidation rate, and hardness of the films at various annealing temperatures.

Annealing temp. (°C)	Element compositions (at%)				Thickness (nm)		Oxidation rate (cm/s <sup>2</sup> )	Hardness (GPa)
	Cr	Al	N	O	CrAlN film	Oxide layer		
RT	28.46	30.93	29.17	11.43	1549.5	-	-	12.47
500	29.22	31.29	25.69	13.80	1492.0	-	-	15.92
600	28.97	30.59	23.21	17.23	1434.0	-	-	11.16
700	25.00	29.48	25.47	20.06	1614.0	-	-	7.23
800	14.09	31.58	24.02	30.31	1360.0	648.0	$1.43 \times 10^{-13}$	0.71
900	11.52	27.86	17.73	42.88	1200.0	1044.0	$3.78 \times 10^{-13}$	0.03

### 3.5 Oxidation kinetics of oxide scale

Oxidation kinetics which is composed of the oxidation rate and the activation energy of the as-deposited and annealed thin films at various temperatures are shown in Table 2. All the oxidation kinetics of the films obey the parabolic law. It is clearly seen that compared with the un-annealed and annealed from 500 to 700°C, the films annealed at 800-900°C have an oxidation rate due to the formation of an oxide layer on the film surface.

In this research work, it was found that the oxidation rate increased from  $1.43 \times 10^{-13}$  to  $3.78 \times 10^{-13}$  cm/s<sup>2</sup> as the annealing temperature reached to 800°C. The apparent activation energy on the coated samples, CrAlN films, oxidized at 800-900°C was determined by the Arrhenius equation. The activation energy of the oxidation was 99.85 kJ/mol. This result was different compared previous study which varied between 174.65-295 kJ/mol, respectively (Drnovšek et al., 2023). It was due to difference of microstructure and element compositions.

### 4. Conclusions

These CrAlN thin films were deposited by reactive magnetron sputtering using an alloy target to investigate the oxidation behavior at annealing temperatures from 500 to 900°C were reported and discussed. The presence of a mixed Cr<sub>5</sub>O<sub>12</sub> and Cr<sub>2</sub>O<sub>3</sub> phase in the samples at an annealing temperature over 700°C has been detected by XRD. A high O concentration from EDX investigation at the same temperature range was found. A needle-like morphology with an increase of oxide layer was identified by FE-SEM at 800 to 900°C. The XRD EDS and FE-SEM results clearly support each other. The decrease of hardness as a result of the oxidation mechanism was observed. The oxidation rate increased to  $3.78 \times 10^{-13}$  cm/s<sup>2</sup>. The oxidation activation energy calculated from the Arrhenius plot was 99.85 kJ/mol. This evidence confirmed that the oxidation behavior was observed and can concluded that the films exhibited an oxidation resistance at 700°C. This result can be indicated that the as-deposited films were also appropriate for tooling applications requiring high temperatures.

### References

- Alaksanasuwan, S., Buranawong, A., & Witit-anun, N. (2022). Structural and oxidation behavior of nanocomposite TiCrN thin films. *Suan Sunandha Science and Technology Journal*, 9(2), 53-62. <https://doi.org/10.53848/ssstj.v9i2.234>
- Alaksanasuwan, S., & Witit-anun, N. (2023). Synthesis and characterization of TiN thin films by DC reactive magnetron sputtering. *Suan Sunandha Science and Technology Journal*, 10(2), 205-212. <https://doi.org/10.53848/ssstj.v10i2.353>
- Anders, A. (2010). A structure zone diagram including plasma-based deposition and ion etching. *Thin Solid Films*, 518(15), 4087-4090. <https://doi.org/10.1016/j.tsf.2009.10.145>
- Anwar, S., Anwar, S., Priyadarshini, B., & Sankar, R. S. (2022). Evaluation of structural and mechanical properties of CrAlN single layer coating deposited by reactive magnetron sputtering. *Materials Chemistry and Physics*, 292, 126873. <https://doi.org/10.1016/j.matchemphys.2022.126873>
- Banakh, O., Schmid, P. E., Sanjines, R., & Levy, F. (2003). High-temperature oxidation resistance of Cr<sub>1-x</sub>Al<sub>x</sub>N thin films deposited by reactive magnetron sputtering. *Surface and Coatings Technology*, 163-164, 57-61. [https://doi.org/10.1016/S0257-8972\(02\)00589-3](https://doi.org/10.1016/S0257-8972(02)00589-3)
- Barshilia, H. C., Selvakumar, N., Deepthi, B., & Rajam, K. S. (2006). A comparative study of reactive direct current magnetron sputtered CrAlN and CrN coatings. *Surface and Coatings Technology*, 201(6), 2193-2201. <https://doi.org/10.1016/j.surfcoat.2006.03.037>
- Buranawong, A., & Witit-anun, N. (2022). Oxidation behavior of nanostructure sputtered titanium nitride thin films. *Current Applied Science and Technology*, 22(6), 1-11. <https://doi.org/10.55003/cast.2022.06.22.015>
- Chim, Y. C., Ding X. Z., Zeng, X. T., & Zhang, S. (2009). Oxidation resistance of TiN, CrN, TiAlN and CrAlN coatings deposited by lateral rotating cathode arc. *Thin Solid Films*, 517(17), 4845-4849. <https://doi.org/10.1016/j.tsf.2009.03.038>
- Drnovšek, A., Kukuruzovic, D., Terk, P., Miletic, A., Cekada, M., Panjan, M., & Panjan, P. (2023). Microstructural, mechanical and oxidation resistance of nanolayer sputter-deposited CrAlN hard coatings. *Coatings*, 13(12), 2096. <https://doi.org/10.3390/coatings13122096>
- He, X.-M., Baker, N., Kehler, B. A., Walter, K. C., Nastasi, M., & Nakamura, Y. (2000). Structure, hardness, and tribological properties of reactive magnetron sputtered chromium nitride films. *Journal of Vacuum Science & Technology A*, 18(1), 30-36.

- He, Y., Gao, K., Yang, H., Pang, X., & Volinsky, A. A. (2021). Nitrogen effects on structure, mechanical and thermal fracture properties of CrN films. *Ceramics International*, 47(21), 30729-30740. <https://doi.org/10.1016/j.ceramint.2021.07.252>
- Kang, Q., Wang, G., Liu, Q., Sui, X., Liu, Y., Chen, Y., Luo, S., & Li, Z. (2021). Investigation for oxidation mechanism of CrN: A combination of DFT and *ab initio* molecular dynamics study. *Journal of Alloys and Compounds*, 885, 160940. <https://doi.org/10.1016/j.jallcom.2021.160940>
- Kayani, A., Buchanan, T. L., Kopczyk, M., Collins, C., Lucas, J., Lund, K., Hutchison, R., Gannon, P. E., Deibert, M. C., Smith, R. J., Choi, D.-S., & Gorokhovskiy, V. I. (2006). Oxidation resistance of magnetron-sputtered CrAlN coatings on 430 steel at 800°C. *Surface and Coatings Technology*, 201(7), 4460-4466. <https://doi.org/10.1016/j.surfcoat.2006.08.049>
- Khamseh, S., & Araghi, H. (2016). A study of the oxidation behavior of CrN and CrZrN ceramic thin films prepared in a magnetron sputtering system. *Ceramics International*, 42(8), 9988-9994. <https://doi.org/10.1016/j.ceramint.2016.03.101>
- Khamseh, S, Nose, M., Kawabata, T., Matsuda, K., & Ikeno, S. (2010). Oxidation resistance of CrAlN films with different microstructures prepared by pulsed DC balanced magnetron sputtering system. *Materials Transactions*, 51(2), 271-276. <https://doi.org/10.2320/matertrans.MC200912>
- Khamseh, S, Nose, M., Kawabata, T., Nagae, T., Matsuda, K., & Ikeno, S. (2010). A comparative study of CrAlN films synthesized by *dc* and *pulsed dc* reactive magnetron facing target sputtering system with different pulse frequencies. *Journal of Alloys and Compounds*, 508(1), 191-195. <https://doi.org/10.1016/j.jallcom.2010.08.042>
- Kim, S., Yoon, H. W., Moon, K., & Lee, C. S. (2021). Mechanical and friction behavior of sputtered Mo-Cu-(N) coatings under various N<sub>2</sub> gas flow using a multicomponent single alloy target. *Surface and Coatings Technology*, 412, 127060. <https://doi.org/10.1016/j.surfcoat.2021.127060>
- Lin, J., Mishra, B., Moore, J. J., & Sproul, W. D. (2008). A study of the oxidation behavior of CrN and CrAlN thin films in air using DSC and TGA analyses. *Surface and Coatings Technology*, 202(14), 3272-3283. <https://doi.org/10.1016/j.surfcoat.2007.11.037>
- Liu, J., Hao, Z., Cui, Z., Ma, D., Lu, J., Cui, Y., Li, C., Liu, W., Xie, S., Hu, P., Huang, P., Bai, G., & Yun, D. (2021). Oxidation behavior, thermal stability, and the coating/substrate interface evolution of CrN-coated Zircaloy under high-temperature steam. *Corrosion Science*, 185, 109416. <https://doi.org/10.1016/j.corsci.2021.109416>
- Mayrhofer, P. H., Willmann, H., & Reiter, A. E. (2008). Structure and phase evolution of Cr-Al-N coatings during annealing. *Surface and Coatings Technology*, 202(20), 4935-4938. <https://doi.org/10.1016/j.surfcoat.2008.04.075>
- Priyadarshini, B., Anwar, S., & Anwar, S. (2023). Substrate temperature: A governing factor for the structural, mechanical and chemical properties of sputtered CrAlN ternary coating. *Thin Solid Films*, 771, 139788. <https://doi.org/10.1016/j.tsf.2023.139788>
- Qi, Z. B., Liu, B., Wu, Z. T., Zhu, F. P., Wang, Z. C., & Wu, C. H. (2013). A comparative study of the oxidation behavior of Cr<sub>2</sub>N and CrN coatings. *Thin Solid Films*, 544, 515-520. <https://doi.org/10.1016/j.tsf.2013.01.031>
- Qu, S.-J., Huang, S.-Q., Guo, C.-Q., Dai, M.-J., Lin, S., Shi, Q., Su, Y.-F., Wei, C.-B., Yang, Z., & Chekan, N. M. (2023). Chromium arc plasma characterization, structure and properties of CrN coatings prepared by vacuum arc evaporation. *Vacuum*, 209, 111796. <https://doi.org/10.1016/j.vacuum.2022.111796>
- Tillmann, W., Dias, N. F. L., & Stangier, D. (2018). Effect of Hf on the microstructure, mechanical properties, and oxidation behavior of sputtered CrAlN films. *Vacuum*, 154, 208-213. <https://doi.org/10.1016/j.vacuum.2018.05.015>
- Wang, L., & Nie, X. (2014). Effect of annealing temperature on tribological properties and material transfer phenomena of CrN and CrAlN coatings. *Journal of Materials Engineering and Performance*, 23, 560-571. <https://doi.org/10.1007/s11665-013-0748-z>
- Xingrun, R., Qinying, Z., Zhu, H., Wei, S., Jiangao, Y., & Hao, C. (2018). Microstructure and tribological properties of CrN films deposited by direct current magnetron sputtering. *Rare Metal Materials and Engineering*, 47(8), 2283-2289. [https://doi.org/10.1016/S1875-5372\(18\)30180-2](https://doi.org/10.1016/S1875-5372(18)30180-2)
- Xingrun, R., Zhu, H., Meixi, L., Jiangao, Y., & Hao, C. (2018). Comparison of microstructure and tribological behaviors of CrAlN and CrN film deposited by DC magnetron sputtering. *Rare Metal Materials and Engineering*, 47(4), 1100-1106. [https://doi.org/10.1016/S1875-5372\(18\)30127-9](https://doi.org/10.1016/S1875-5372(18)30127-9)

- Zhang, M, Lin, G., Lu, G., Dong, C., & Kim, K. H. (2008). High-temperature oxidation resistant (Cr, Al)N films synthesized using pulsed bias arc ion plating. *Applied Surface Science*, 254(22), 7149-7154.  
<https://doi.org/10.1016/j.apsusc.2008.05.293>
- Zhu, M., Li, M., & Zhou, Y. (2006). Oxidation resistance of  $\text{Cr}_{1-x}\text{Al}_x\text{N}$  ( $0.18 \leq x \leq 0.47$ ) coatings on K38G superalloy at 1000–1100°C in air. *Surface and Coatings Technology*, 201(6), 2878-2886.  
<https://doi.org/10.1016/j.surfcoat.2006.05.045>